WC3
14:30 – 14:45

Metal-oxide-silicon nanophotonics: an efficient integration of plasmonic nano-slots with silicon waveguides.

Cécile Delacour*, Philippe Grosse, Jean Marc Fedeli, Alexei Chelnokov*
CEA LETI, MINATEC
17 rue des Martyrs,
38054 Grenoble, France.
cecile.delacour@cea.fr, alexei.tchelnokov@cea.fr

Sylvain Blaize, Aurélien Bruyant, Rafael Salas-Montiel, Gilles Lerondel
Laboratoire de Nanotechnologie et d'Instrumentation Optique, Institut Charles Delaunay,
CNRS-FRE 2848, Université Technologique de Troyes,
10010 Troyes, France

***Abstract*— We demonstrate key elements of future plasmonic guided optics integrated with CMOS-compatible silicon photonics. Very efficient coupling is provided with metal nano-slot waveguides exhibiting unexpectedly low propagation losses and a broadband sub-50 nm optical confinement.**

Keywords: surface plasmon polariton, metallic slot waveguides, co-directional couplers, silicon photonics, plasmonics, integrated optics.

I. INTRODUCTION

Coupling plasmonic and silicon photonics is the best way to bridge the size gap between macroscopic optics and nano-devices in general and especially nanoelectronic devices. Being very compact [1,2,3], plasmonic waveguides should provide for efficient optical coupling to truly nanoscopic devices [4]. They can guide both light and electrical current. In addition, high optical confinement can significantly decrease the threshold of non-linear effects for all-optical switching applications [5]. Here, we show that highly efficient plasmonic waveguides and non-resonant optical couplers between metallic and silicon optical waveguides can be achieved in a fully CMOS-compatible way.

II. DEVICE CONFIGURATION AND FABRICATION

We explore copper based slotline waveguides. The slotline configuration appears to be the most promising since it can be fabricated using a single lithography step. Strong confinement (50x50 nm²) inside the slot with very little outside spreading was predicted theoretically [6]. And the guiding metallic side walls can act as contact electrodes to implement opto-electrical devices [7,8]. The copper was chosen since it is accepted in the CMOS fab facilities.

Due to the difference in the mode sizes between the silicon and the slotline waveguides, a direct butt coupling would be prohibitively inefficient Instead of adapting the mode sizes, we choose to use directional coupling [9,10] between Si and metallic slotline waveguides, both of constant cross section. The principle of directional coupling between two waveguides is widely known and used [11] for dielectric waveguides. The directional couplers are non-resonant and highly efficient even in presence of fabrication imperfections.

The overall sketch of the plasmonic photonic hybrid structure studied in this paper is shown in the Figure 1. It includes a plasmonic slotline waveguide composed of two copper strips separated with a nanoscale slot. The slotline waveguide is in a close vicinity of an interrupted silicon ridge monomode waveguide with two overlapping areas respectively for front and back end coupling. The whole structure is embedded in silica. The overlapping area in the direction of the propagation defines the coupling length over which the power exchange between the two waveguides is expected to occur.

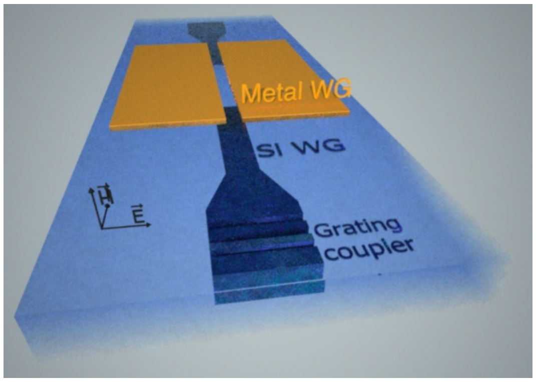

Figure 1. A sketch of the hybrid optical chip showing the metallic slotline coupled to silicon ridge waveguides. The slotline consist of two coplanar metallic strips spaced to form the slotline. The metallic and silicon waveguides are vertically spaced. Coupling occurs at the overlapping areas. A diffraction grating is used to couple the light from an optical fibre to the silicon waveguide in the spectral range of 1.3-1.5 µm.

We fabricated the devices in a 200-mm wafer CMOS front end fabrication facility using 193 nm optical projection

---

This work was partially financed by the French National Research Agency (ANR) through Carnot funding.

978-1-4244-6346-6/10/$26.00 ©2010 IEEE

lithography and metals that are non contaminant for the Si microelectronics. The scanning electron microscope images of the fabricated devices are shown in the Figure 2.

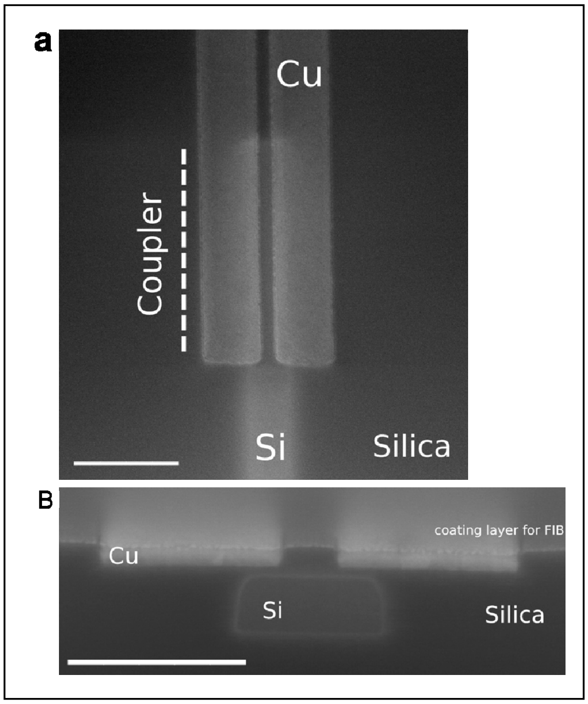

Figure 2. Scanning electron micrographs of the fabricated devices. a) Top view of the coupler showing the copper slotline waveguide and the silicon waveguide buried underneath. b) Cross-section of the coupler. The scale bars are 1 µm.

III. DEVICE CHARACTERISATIONS

The transmission of the devices was measured as function of the overlapping length around the wavelength of 1.55 µm using both wide band superluminescent light emitting diodes (SLED) and a laser, all interfaced via monomode fibres. An automated probe station was used for systematic device characterization. The SLED measurements confirmed the wide non-resonant spectral operation of the structures. The experimental data (not shown here) unambiguously confirmed the variation of the coupling efficiency with the coupler length predicted by the co-directional coupling model.

The Figure 3 shows the statistics of the transmission efficiency of the "Si waveguide<>coupler<>metal slotline<>coupler<>Si waveguide" structures. The statistics was obtained on one 200 mm wafer for fixed lengths of the slotline and of the couplers (7.8 µm slotline including two 0.9 µm long couplers). More than 30% of the measured devices exhibit the overall transmission of better than 40%. We consider these unexpectedly good values as being compatible with future practical use of plasmonic devices.

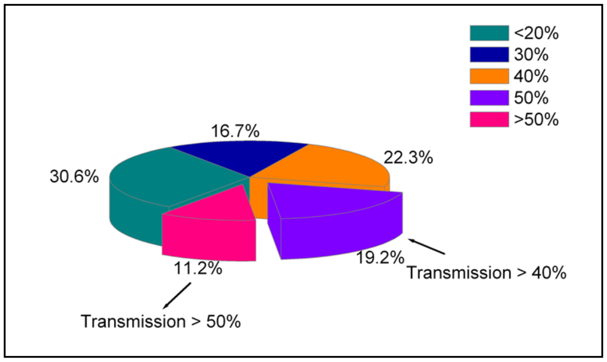

Figure 3. Statistics of Si-Coupler-Slotline-Coupler-Si transmissions measured with automated prober using SLED source (λ0=1.55 µm, FWHM=50nm). The overall copper slotline length is of 7.8 µm, including two couplers of 0.9 µm length each.

To confirm the results of macroscopic characterizations, we analysed the operation of the couplers/guides combinations at a wavelength scale using transmission-based near-field scanning optical microscope operating at 1.55 µm. The intensity of the optical near-field reported in the Figure 4a clearly shows the surface plasmon polariton supported by the metal-dielectric-metal interfaces inside the slotline. Modulation of the intensity occurs with a period of 420nm, suggesting the reflection of the uncoupled light at the ends of the slot in agreement with an effective index of the surface plasmon of about 1.85. This very interesting result underlines the low loss of the copper waveguide. Optical and material properties of the high quality copper film are currently further investigated. The signal related to the photonic mode of the Si waveguide is weaker than that of the Cu waveguide, as the silicon waveguide is embedded much deeper into the silica. Our simulations of the tested device (Fig. 4b) predict that almost 60 % of incident power is transmitted to the output waveguide with monochromatic source at 1.55 µm, in agreement with experimental data (Fig. 3).

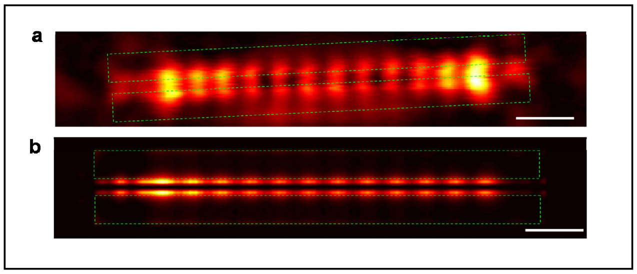

Figure 4. Near field characterization. a) Optical near-field micrograph clearly shows the plasmonic mode confined in the slot. The two brightest regions correspond to the input and output coupling to the silicon waveguides. Magnitude of the field oscillates along the propagation direction with a period of 420nm. The silicon waveguides are buried so their signal is lower. b) Numerical simulation (FDTD) of the tested device showing the steady state of the energy density of the electrical field. For both measurement and simulation a monochromatic source of λ0=1.55 µm was used. Scale bars are 1µm.

IV. CONCLUSION

We demonstrate highly efficient plasmonic devices technologically compatible with both Si photonics and Si electronics. The two most essential bricks of plasmonic integrated optics (waveguide and coupler) are integrated with traditional silicon photonic waveguides and operated at the optical telecommunications wavelengths.

The present demonstration enables more complex integrated plasmonic devices as the already suggested plasmonic based modulators [8,12] and sources [13,14]. We currently investigate the implementation of other integrated plasmonic/Si devices (e.g. Fig. 5) Operation of other CMOS-compatible metals is also being tested in similar plasmonic structures.

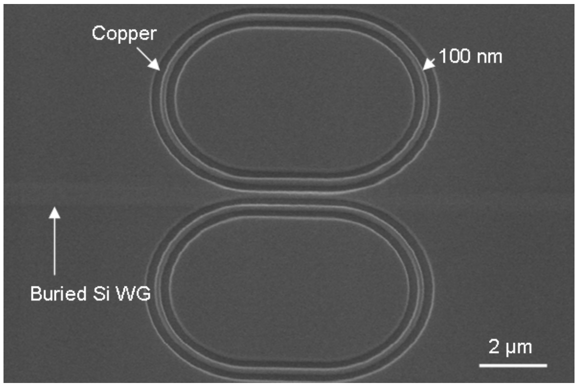

Figure 5. Example of more complex Si-integrated plasmonic devices: coupled copper ring resonators coupled to a buried Si ridge waveguide. Co-planar copper slotlines with 100 nm wide slot and 300 nm wide side metal ribbons.

[1] Zia, R., Schuler, J.A., Chandran, A. & Brongersma, M.L. Plasmonics: the next chip-scale technology. Mater. Today, vol. 9, pp. 20-27, 2006.

[2] Ozbay, E. Plasmonics: merging photonics and electronics at nanoscale dimensions. Science vol. 311, pp. 189-193, 2006.

[3] Barnes, W. L., Dereux, A. & Ebbesen, T. W. Surface plasmon subwavelength optics. Nature, vol. 424, pp. 824-830, 2003.

[4] Akimov, A. V. et al. Generation of single optical plasmons in metallic nanowires coupled to quantum dots. Nature, vol. 450, pp. 402-406, 2007.

[5] Koos, C. et al. All-optical high-speed signal processing with silicon-organic hybrid slot waveguides. Nature photon. vol. 3, pp. 216-219, 2009.

[6] Veronis, G. & Fan, S. Guided subwavelength plasmonic mode. Opt. Lett. 30, pp. 3359-3361, 2005.

[7] Cai, W., White, J.S. & Brongersma, M. Compact, high-speed and power-efficient electrooptic plasmonic modulator. Nano Lett. 9, 4403-4411 (2009).

[8] Cohen G.M. et al.. Nanowire metal-oxide-semiconductor field effect transistor with doped epitaxial contacts for source and drain, Appl. Phys. Lett., vol. 90, 233110, 2007.

[9] Yariv, A. Coupled-mode theory for guided-wave optics, J. Quantum Electron. vol. .9, pp. 919-933, 1973.

[10] Huang, W.P. Coupled-mode theory for optical waveguides: an overview, J. Opt. Soc. Am. A, vol. 11, pp. 963-983, 1994.

[11] Gramotnev, D.K., Vernon, K.C., Pile, D.F.P. Directional coupler using gap plasmon waveguides, Appl. Phys. B, vol. 93, pp. 99-106, 2008.

[12] Dionne, J.A. et al. Plasmostor: a metal oxide Si field effect plasmonic modulator. Nano Lett. , vol. 9, pp. 897–902, 2009.

[13] Dionne, J. A. et al. Silicon-based plasmonics for on-chip photonics, Journal of Selected Topics in Quantum Electronics, vol. 16, pp. 295-306, 2010.

[14] Hryciw, A., Jun, Y.C. & Brongersma, M.L. Nature Mater., vol. 9, pp. 3-4, 2010.